tvst

Article

Quantitative Fundus Autofluorescence in the Developing and Maturing Healthy Eye

Carla Pröbster[1], Ioana-Sandra Tarau[1], Andreas Berlin[1], Nikolai Kleefeldt[1], Jost Hillenkamp[1], Martin M. Nentwich[1], Kenneth R. Sloan[2], and Thomas Ach[1,3]

[1] Department of Ophthalmology, University Hospital Würzburg, Würzburg, Germany
[2] Department of Ophthalmology, University of Alabama at Birmingham, Birmingham, AL, USA
[3] Department of Ophthalmology, University Hospital Bonn, Bonn, Germany

Correspondence: Thomas Ach, University Hospital Bonn, Department of Ophthalmology, Ernst Abbe Straße 2, Bonn, 53127, Germany. e-mail: thomas.ach@ukbonn.de

Received: November 12, 2020
Accepted: January 10, 2021
Published: February 11, 2021

Keywords: quantitative fundus autofluorescence; children; adolescence; retinal imaging; retina; retinal pigment epithelium; lipofuscin; melanolipofuscin; melanosome

Citation: Pröbster C, Tarau I-S, Berlin A, Kleefeldt N, Hillenkamp J, Nentwich MM, Sloan KR, Ach T. Quantitative fundus autofluorescence in the developing and maturing healthy eye. Trans Vis Sci Tech. 2021;10(2):15, https://doi.org/10.1167/tvst.10.2.15

Purpose: Quantitative fundus autofluorescence (QAF) enables comparisons of autofluorescence intensities among participants. While clinical QAF reports mostly focused on the healthy and diseased adult retina, only very limited data of QAF in the maturing eye are available. Here, we report QAF in a large cohort of healthy children.

Methods: In this prospective monocentric cross-sectional study, 70 healthy Caucasian children (5–18 years) were multimodal imaged, including QAF and spectral domain optical coherence tomography. QAF and retinal thicknesses were measured at predefined locations (along horizontal meridian; Early Treatment Diabetic Retinopathy Study [ETDRS] grid) and correlated using custom written Fiji plugins. Standard retinae for different age groups were generated.

Results: Fifty-three participants were included. QAF was low in childhood but increased steadily ($P < 0.001$), also at the fovea ($P < 0.001$), with no gender differences ($P = 0.61$). The QAF distribution was similar to adults showing highest values superior-temporally. At individual points, retinal thickness remained stable, while using the ETDRS pattern, the retinal pigment epithelium (RPE) thickness increased significantly with aging. Standard QAF retinae of age groups also showed an increase with aging.

Conclusions: QAF can be reliably performed in young children. Function–structure correlation showed a thickening of the RPE and an increasing QAF with aging, probably related to the histologic low number of RPE autofluorescent granules at a younger age but further deposition of these granules during maturation. Standard retinae help to distinguish abnormal QAF in the diseased retina of age-matched patients.

Translational Relevance: Our data bridge the gap between preclinical QAF and clinical data application and structural OCT correlation in children.

Introduction

Fundus autofluorescence (FAF) imaging has been a noninvasive, safe, and fast technique for functional imaging of the human retina for over 25 years.[1,2] It has been widely accepted and is used for the diagnosis and therapy monitoring in hereditary and age-related retinal diseases, as well as an imaging modality in multiple clinical trials.

FAF has its origin in fluorophores (e.g., bisretinoids and other currently unknown compounds) in the outer retina (photoreceptors, retinal pigment epithelium [RPE]), with RPE being the major contributor.[2,3] Several histologic studies showed that lipofuscin and melanolipofuscin granules within the RPE are key for the FAF signal.[4,5] Most of these granules start to accumulate within RPE cells in the second decade of life and are traceable into advanced age.[4] However, there are very limited data on the accumulation of granules with autofluorescent properties in the retina and RPE of children and adolescents.

Until recently, FAF imaging enabled only qualitative description of FAF patterns due to varying

laser power or detector sensitivity between imaging sessions and patients. In 2011, Delori et al.[6] introduced a clinical-experimental method, quantitative FAF imaging (QAF), enabling quantitative measurements of the autofluorescence intensities. In the QAF setup, an internal reference is exposed parallel to the retina, and the gray values of the image can then be normalized to the internal reference. While QAF has shown its clinical applicability in several studies both in healthy participants[6–8] and in patients with retinal disorders,[9–11] only marginal QAF data of the developing and maturing eye are available.[7]

The goal of our study was to quantitatively analyze the FAF in a large cohort of healthy Caucasian children and young adolescents. QAF data are reported for each individual and as standard retina for each decade. Our findings will increase the knowledge on FAF development in the young retina and also serve as a basis for the comparison of pathologic QAF signals in the diseased young eye.

Methods

Study Population

Seventy healthy children (age range 5–18 years, all Caucasians) were recruited from the Department of Ophthalmology, University Hospital Würzburg, between April 1, 2018, and March 30, 2019. Participants were asked to participate as part of their clinical consultation. After written consent (legal custodians) and the explanation of the advantages and possible side effects of this study, participants were included. All study procedures followed the tenets of the Declaration of Helsinki, and the University of Würzburg's Ethics Committee approved this study (#97/17). Participants received no financial compensation.

Inclusion criteria were clear optical media (cornea, lens, vitreous body). Exclusion criteria were a family history of inherited retinal disease, presence of acute or previous retinal/macular pathologies, history of intraocular surgeries, or inability to follow the instructions during the multimodal retinal imaging session. In addition, participants were excluded if images showed low image quality (see below) due to insufficient fixation, eyelid interference, or uncompleted image series.

Ophthalmologic examination included best-corrected visual acuity, slit-lamp biomicroscopy of the anterior segment, and dilated indirect fundoscopy (1% cyclopentolate or 0.5% tropicamide).

Imaging

All participants were examined following protocols and recommendations from previous QAF studies.[7] Briefly, each participant´s corneal curvatures were measured (IOLMaster 500; Carl Zeiss AG, Oberkochen, Germany), followed by a macular spectral domain optical coherence tomography (SD-OCT) scan (20 × 20°, 49-line scan, average of 35 frames for each line scan, distance between line scans 120 µm), including an infrared image using the Spectralis OCT (Heidelberg Engineering, Heidelberg, Germany), and QAF with a modified HRA2 device (Heidelberg Engineering).

Acquisition of the QAF Image

All QAF fundus imaging was performed by one trained operator (CP). Camera and device´s internal software settings were excitation 488 nm, emission 500 to 750 nm, 30° × 30° field, and high-speed mode. Participants' pupil diameter had to be at least 6 mm. Focus and detector sensitivity were adjusted for each individual, and images were acquired with central macula in focus and the gray levels not exceeding the linear range of the detector. The fundus was then illuminated with blue light (488 nm excitation) for at least 20 seconds to ensure the photoreceptor´s photopigment bleaching.[6,7]

At least two QAF image series consisting of 12 single frames each were taken. Between the two series, participants were asked to close their eyes and relax before the camera was realigned. Immediately after image acquisition, both series were checked for quality (images correctly centered on the fovea, evenly illuminated posterior pole, no eyelid interference), and low-quality frames were removed using the device´s internal software (HEYEX; Heidelberg Engineering). The remaining frames (at least nine) were averaged and saved as a raw image. This imaging procedure was then repeated with the fellow eye. From each participant, the eye with the best QAF image quality was included. If images from both eyes showed equal quality, the left eye was chosen since all data from our customized Fiji plugins report and plot left eye data. Subsequently, right eyes, if included, were converted to left eyes upfront. All Spectralis and HRA2 images were adjusted using the participant's individual corneal c-curves enabling calculation of axial length indirectly (with corneal curvatures being the most substantial

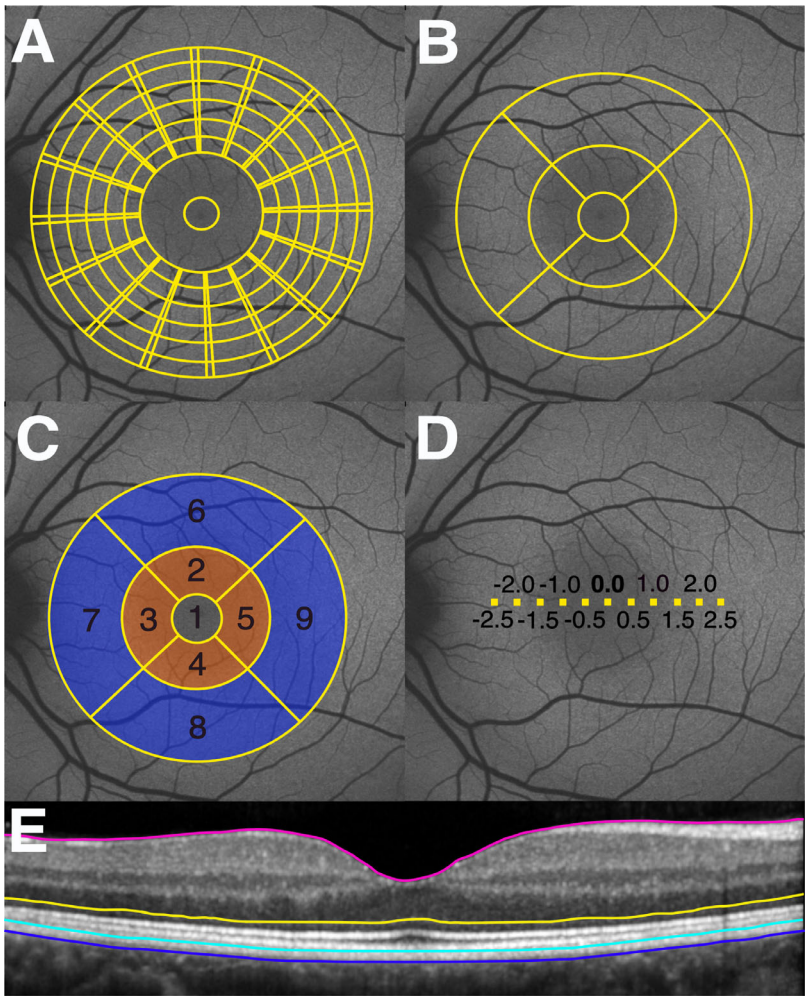

Figure 1. QAF analysis grids and retinal thickness measurements. The QAF97 (**A**) analysis pattern is centered on the fovea, but total grid size slightly varies from participant to participant since grid diameter is a function of distance from fovea to edge of optic nerve head. The ETDRS pattern (**B**) is centered on the fovea and has defined ring sizes (diameters: 1, 3, and 6 mm). Retinal layer thicknesses were measured within the ETDRS subdivisions (**C**) and at certain distances along a horizontal meridian (11 points, distance 0.5 mm) (**D**), both centered on the fovea. The internal limiting membrane (ILM, *pink*), the external limiting membrane (ELM, *yellow*), RPE (*turquoise*), and Bruch membrane (*blue*) are highlighted (**E**). The thickness of the whole retina was measured between ILM and RPE/Bruch membrane, the inner retina between ILM and ELM, and the outer retinal thickness between ELM and RPE/Bruch membrane.

factor), which also affects scaling of the image and, subsequently, QAF values.[6]

Image Analysis

Custom-written Fiji plugins (available upon request) were used for image processing, as previously reported.[8] Briefly, exported QAF raw images were adjusted for the device-specific reference calibration factor (as delivered by the manufacturer) and the participant´s age-related media opacity. QAF images were then converted to colored 8-bit images (QAF values limited to [0 to 511] and scaled to [0 to 255]).[8]

Image analysis was based on a fovea-centered pattern. For this purpose, within the SD-OCT macula volume scan, the exact location of the fovea (maximum elevation of the external limiting membrane and deepest foveal depression) was determined. Since the SD-OCT volume scan comes with a simultaneously captured infrared (IR) image, the exact position of the fovea could be transferred to the en face IR image. Then, the QAF image was registered against and aligned with the IR image by specifying two landmarks (vascular bifurcations) visible in both images, followed by a transformation including translation, rotation, and uniform scaling.[8]

QAF Analysis and Structural Correlation with SD-OCT

For QAF analysis, two fovea-centered patterns, QAF97 and Early Treatment Diabetic Retinopathy Study (ETDRS) grid, were used (Fig. 1). While the ETDRS grid has defined ring widths (diameters: 1, 3, 6 mm), the widths of the previously introduced QAF97 are adapted to the individual fovea–edge of optic nerve head (ONH) distance.[8] The edge of the ONH was determined in the IR image for each individual.[8] The mean, maximum, minimum, and standard deviation of QAF values and the number of pixels for each segment of the appropriate pattern were reported in a tab-delimited text file. Mean QAF values were calculated by averaging the particular segments of each grid (QAF97: 96 segments + fovea; Fig. 1). Herein, we report QAF97 (except fovea) and QAF_{fovea}. QAF data from individual participants were combined to plot standard retina maps: the mean QAF values and the standard deviation of QAF values for each pixel at a given distance and orientation from the fovea for two groups (5–10 years and 11–18 years).

To combine functional (QAF) and structural (SD-OCT) data, QAF values from each segment of the ETDRS grid or from focal points along the horizontal meridian were correlated with the corresponding retinal thicknesses, as measured in SD-OCT. In detail, for the ETDRS grid, retinal layers in all B-scans were automatically segmented using the device´s internal software and manually corrected if necessary, and mean retinal thicknesses of each segment are reported. Mean QAF values for each ETDRS segment were calculated within the QAF image and the overlying ETDRS grid.

In addition, for a subtler analysis, retinal thicknesses and QAF values at 11 points along the horizontal meridian through the fovea (distance between points 0.5 mm; centered on the fovea; Fig. 1) were measured using a custom Fiji plugin (QAF_XML_Grids, version 1.0.1; available upon request). At each point, the internal limiting membrane, the external limiting membrane, and Bruch membrane were manually marked with computer assistance, based on the intensity profiles of the B-scan reflectivity (Fig. 1), and thicknesses (whole retina, inner retina [inner limiting membrane – external limiting membrane], outer retina [external limiting membrane – RPE/Bruch membrane band]) were calculated. Mean QAF values are reported (mean from an area of 5 × 5 pixels) from the corresponding eleven locations within the QAF image.

In addition, the RPE thickness within each segment of the ETDRS grid was measured using the manufacturer´s software (HEYEX; Heidelberg Engineering) and manually corrected when necessary.

Statistical Analysis

Data collection, organization, and analysis were performed using SPSS statistics software package (IBM SPSS 26.0; IBM Corporation, Armonk, NY, USA). Categorical variables are presented as numbers and percentages, and continuous variables are expressed as means ± SDs. $P < 0.05$ was considered statistically significant. Intraclass correlation coefficients were computed to determine the image reading agreement of retinal thickness measurements. Assumptions of normally distributed continuous variables were tested using quantile-quantile plots and Kolmogorov-Smirnov and Shapiro-Wilk tests. The Mann-Whitney *U*-test or *t*-test for independent samples was applied for mean values of retinal thickness and mean values of QAF97. An independent two-sample *t*-test was used to investigate gender differences. The correlation between retinal thickness and mean QAF97 was calculated using Spearman's rank correlation coefficient (*rs*) or Pearson product-moment correlation coefficient (*r*). Multiple linear regression models were used to predict the effect of age and retinal thickness on QAF.

Results

Of 70 initially examined participants, 17 had to be excluded for further analysis due to poor image quality. For final analysis, 53 eyes from 53 individuals (27 females [50.9%]) were included. Twenty-five were 10 years or younger (mean 7.5 ± 1.5 years), and 28 were between 11 and 18 years (mean 13.9 ± 2.3 years). Table summarizes the detailed demographic information for all participants.

The QAF97 (except fovea) intensities increased statistically significantly with age ($P < 0.001$). Mean QAF97 at age 5 years was 47.5 [QAF arbitrary units (a.u.)], and QAF97 increased by 5.0 ± 0.8 [QAF a.u.] per life year (Fig. 2). Gender had no significant effect on the QAF values ($P = 0.61$). The autofluorescence signal at the fovea (QAF_{fovea}) was generally low; however, there was also a statistically significant increase of QAF intensities at the fovea with age ($P < 0.001$), starting with a mean QAF_{fovea} of 33.9 [QAF a.u.] at age 5 years and an annual increase by 2.2 ± 0.6 [QAF a.u.] (Fig. 2). QAF values at the fovea showed no gender differences ($P = 0.887$).

Table. Participant Demographics

Participant ID	Age, y	Sex	Eye	Visual Acuity	QAF97, Mean ± SD	QAF_{fovea}, Mean ± SD
0006	5	F	OD	20/20	75.8 ± 10.8	46.9 ± 6.4
0039	5	M	OD	20/30	58.6 ± 14.0	57.2 ± 6.6
0046	5	F	OD	20/20	54.3 ± 6.5	34.1 ± 5.8
0031	6	F	OD	20/20	75.9 ± 9.8	46.9 ± 6.2
0052	6	F	OD	20/15	101.1 ± 16.6	56.2 ± 8.9
0061	6	F	OD	20/50	73.4 ± 9.0	46.5 ± 5.2
0062	6	M	OS	20/15	106.0 ± 13.0	63.2 ± 9.8
0012	7	F	OD	20/20	68.6 ± 13.1	44.9 ± 5.5
0021	7	F	OS	20/20	103.2 ± 15.2	56.4 ± 5.6
0022	7	M	OS	20/25	64.8 ± 11.8	54.7 ± 7.7
0027	7	M	OD	20/15	100.0 ± 18.7	55.8 ± 10.0
0053	7	F	OD	20/15	97.9 ± 12.7	57.1 ± 8.6
0063	7	M	OD	20/20	93.9 ± 10.3	56.5 ± 6.1
0070	7	M	OD	20/20	94.7 ± 11.4	45.0 ± 8.8
0007	8	M	OD	20/40	39.1 ± 5.8	16 ± 3.7
0028	8	M	OD	20/15	72.5 ± 8.8	31.8 ±5.6
0037	8	M	OD	20/15	67.5 ± 10.4	38.4 ± 5.4
0010	9	M	OD	20/20	90.5 ± 13.7	50.4 ± 9.7
0011	9	F	OD	20/20	81.5 ± 11.5	56 ± 7.0
0029	9	F	OS	20/15	134.1 ± 21.2	94.1 ± 14.6
0040	9	M	OD	20/20	84.6 ± 11.3	44.0 ± 8.2
0041	9	M	OD	20/20	67.9 ± 6.3	35.4 ± 4.9
0045	10	M	OD	20/15	116.9 ± 27.0	60.8 ± 9.5
0048	10	F	OD	20/20	84.5 ± 9.0	48.7 ± 10.3
0064	10	M	OS	20/15	94.8 ± 10.0	57.0 ± 8.1
0019	11	M	OS	20/30	106.4 ± 14.0	49.1 ± 12.1
0038	11	M	OD	20/20	98.8 ± 15.4	40.8 ± 7.8
0044	11	M	OD	20/15	105.4 ± 9.6	48.7 ± 8.3
0047	11	M	OD	20/15	99.2 ± 12.7	55.8 ± 8.0
0057	11	M	OD	20/20	126.8 ± 20.0	55.9 ± 9.5
0018	12	M	OD	20/20	119.4 ± 15.6	63.7 ±8.3
0025	12	F	OD	20/20	68.9 ± 10.3	33.9 ± 6.7
0030	12	F	OD	20/15	99.3 ± 9.4	61.4 ± 8.1
0036	12	F	OD	20/15	109.9 ± 14.8	63.7 ± 10.5
0054	12	M	OD	20/16	125.5 ± 15.4	93.4 ± 8.2
0002	13	F	OD	20/20	105.7 ± 9.8	56.5 ± 8.4
0015	13	F	OD	20/20	106.1 ± 16.2	47.4 ± 5.6
0042	13	F	OD	20/20	132.8 ± 14.8	66.4 ± 11.0
0026	14	F	OS	20/15	112.0 ± 15.6	55.8 ± 11.8
0050	14	M	OD	20/13	163.5 ± 19.7	78.4 ± 11.0
0014	15	F	OD	20/15	70.4 ± 20.9	30.4 ± 6.9
0032	15	M	OD	20/15	162.6 ± 19.5	85.6 ± 15.1
0058	15	F	OS	20/20	127.0 ± 20.7	81.2 ± 13.6
0069	15	F	OD	20/20	116.3 ± 16.7	91.3 ± 9.7
0003	16	F	OD	20/20	98.3 ± 18.2	44.2 ± 9.6
0013	16	M	OS	20/30	113.6 ± 20.1	68.1 ± 7.8
0065	16	F	OS	20/25	130.0 ± 12.8	70.9 ± 17.3
0066	16	F	OS	20/15	133.3 ± 19.7	82.3 ± 20.7
0016	17	M	OD	20/15	138.2 ± 14.3	54.4 ± 9.5
0023	17	M	OD	20/20	155.8 ± 17.4	82.4 ± 20.0
0043	17	F	OD	20/25	131.4 ± 17.5	85.9 ± 17.1
0055	17	F	OS	20/20	139.8 ± 24.0	68.0 ± 10.7
0067	18	M	OD	20/15	113.1 ± 17.6	69.1 ± 11.8

Age is presented in years and visual acuity in Snellen. QAF values are presented as arbitrary units. QAF97: mean of the 96 extrafoveal segments. OD, right eye; OS, left eye.

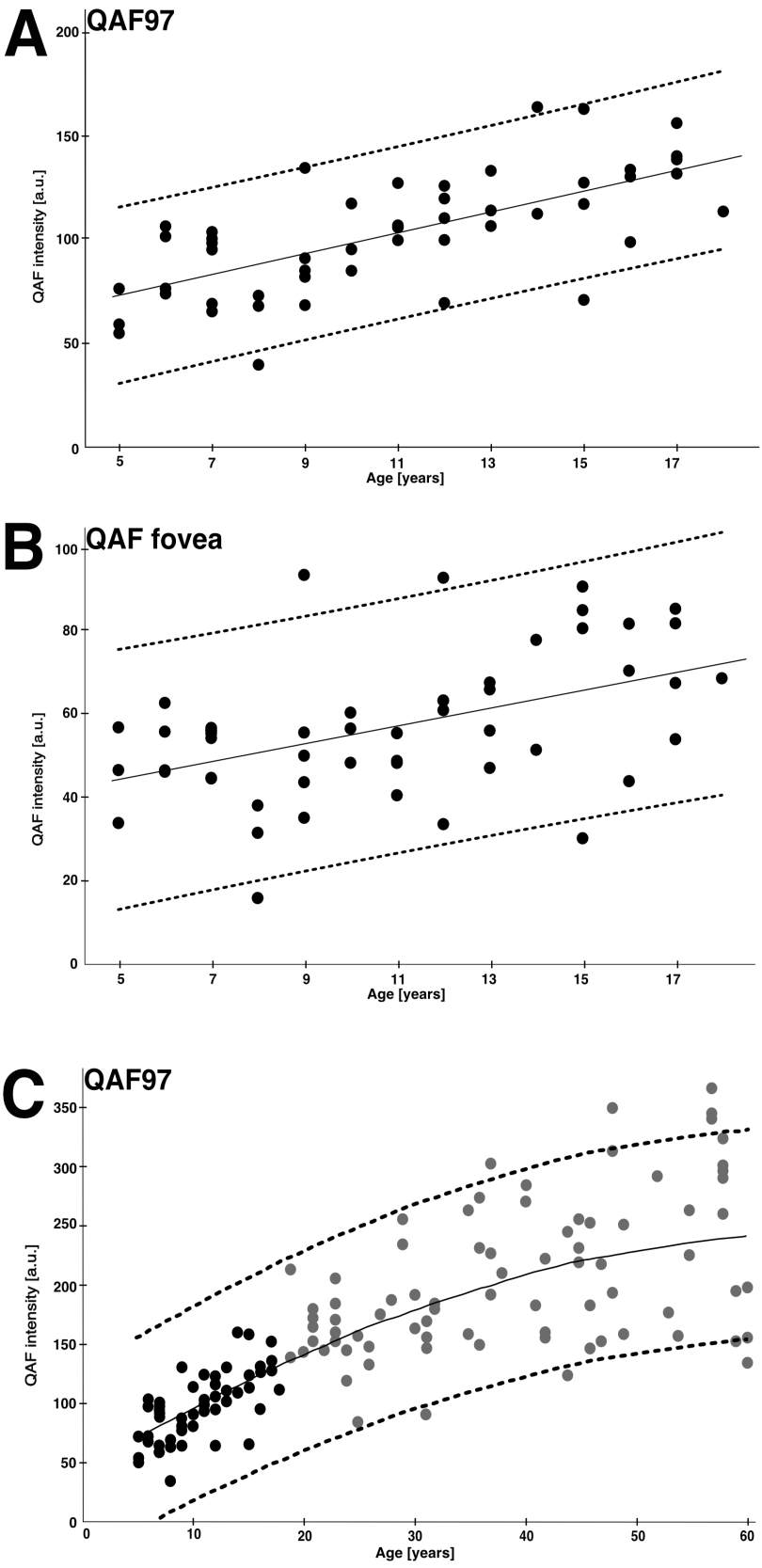

Figure 2. QAF97 and QAF_{fovea}. Total QAF97 (except fovea) values (**A**) and QAF values of the fovea (**B**) of all 53 participants are plotted as a function of age. Linear trend lines (solid lines) and ± 95% confidence limits (dashed lines) are shown. (**C**) QAF in our healthy cohort for each participant aged between 5 and 60 years. The *black dots* represent the children of the current study, while the *gray dots* represent participants aged 19 to 60 years, adopted from our previous study in healthy controls.[8]

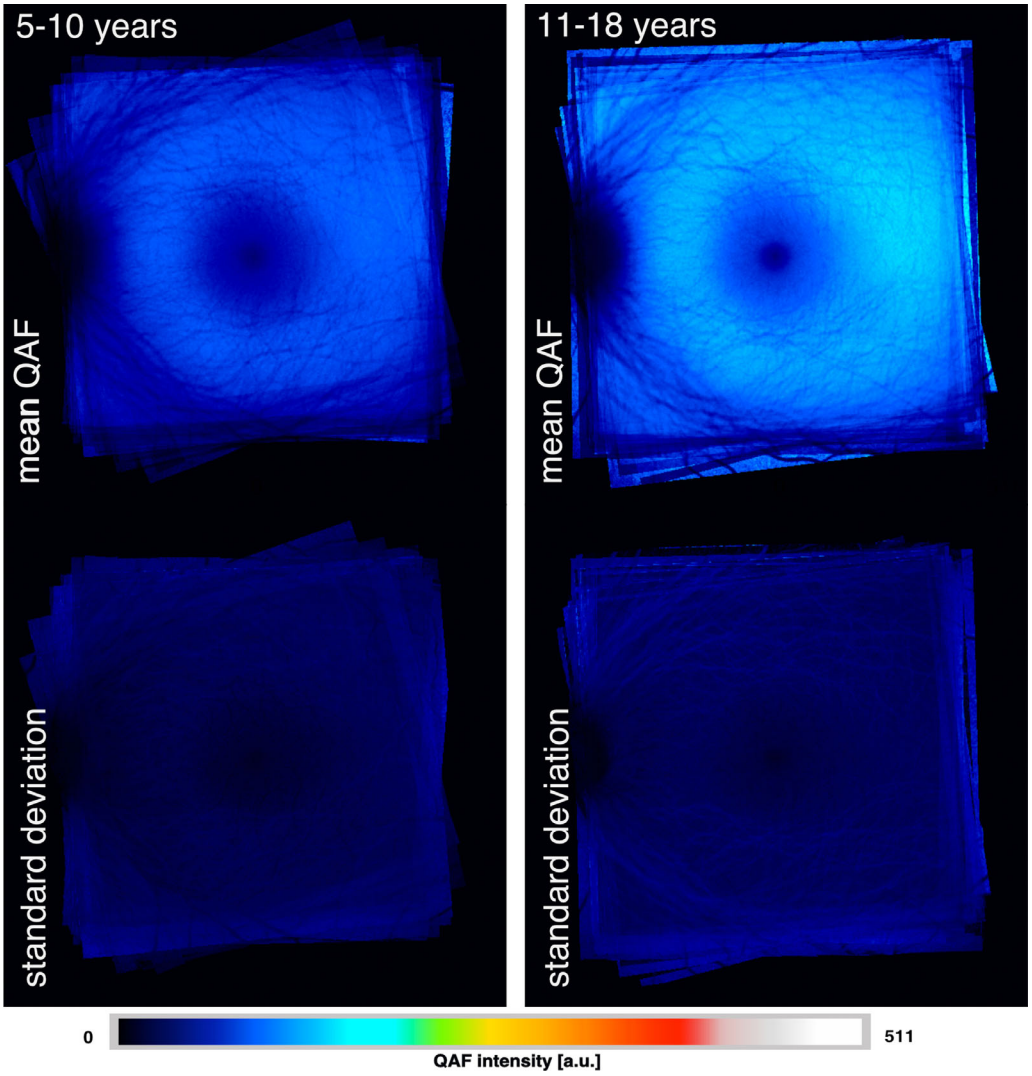

Figure 3. Standard retinae of two age groups. The standard retina represents the mean QAF value for each pixel at a given distance and orientation from the fovea of the corresponding participants for the two groups, aged 5 to 10 and 11 to 18 years. The color-coded QAF standard retinae show an increase with age.

Similar results with an increase in QAF can also be observed using the original QAF8 grid in our cohort (data not shown).[6,7]

Standard Retinae

For each age group (5–10 years, n = 25; 11–18 years, n = 28), a standard retina was generated, showing the mean QAF value for each pixel throughout the posterior pole. (Fig. 3). The qualitative autofluorescence (AF) distribution was identical in both age groups. Highest QAF intensities were found at the parafovea, with maximum values superior temporal. This pattern of AF distribution was detectable even in the youngest of our participants. With increasing age, there was a general increase in fundus autofluorescence across the posterior pole, maintaining the pattern of highest AF intensity at the parafovea (Fig. 3). The segments with the highest QAF values are shown in Figure 4.

SD-OCT Thickness and Correlation with QAF

Evaluating the horizontal meridian, the thickness of the whole retina increased significantly with age ($P < 0.05$) at the fovea but not outside the fovea (Supplementary Table S1). Boys had significantly higher retinal thicknesses at most locations along the horizontal meridian (Supplementary Table S1).

The thickness of the inner retina increased significantly at the fovea ($P = 0.002$) and 1.5 mm from the foveal center ($P = 0.001$). The inner retina of male

Figure 4. Segments with highest QAF values. For both age groups, the segments with the five highest QAF values are plotted. These segments are located at the temporal macula.

participants was significantly thicker at 0.5 mm and 1.0 mm at both sides from the fovea (0.5 mm nasal from fovea: $P = 0.004$; 1.0 mm nasal from fovea: $P = 0.002$; 0.5 mm temporal from fovea: $P = 0.001$; 1.0 mm nasal from fovea: $P = 0.001$; Supplementary Table S1).

The thickness of the outer retina revealed no age- or gender-related changes (Supplementary Table S1).

Similar results were found using the ETDRS grid (Supplementary Table S2). The thickness of the whole retina did not markedly change with age (unspecific significant change in ETDRS segment 8, $P < 0.05$). Boys had significantly higher retinal thicknesses compared to girls. The thickness of the outer retinal layers did not change with age. Differences between genders could only be seen at segments 7 ($P < 0.05$) and 8 ($P < 0.05$). However, for ETDRS ring 1 ($P <$ 0,01) and segments 1 ($P < 0.05$), 2 ($P < 0.01$), 3 ($P <$ 0.01), and 4 ($P < 0.05$) there was a significant increase of RPE thickness with age. Gender had no significant effect on RPE thickness (Supplementary Table S2).

QAF and Correlation with Retinal Thickness

QAF increased significantly at all 11 points on the horizontal meridian with age, with the exception of the central point at the fovea (Fig.5; Supplementary Table S1). There was a significant positive and negative correlation in the focal retinal thickness measurements at the nasal parafovea (1.5 mm from foveal center), showing an increase of QAF with increasing outer retinal thickness and decrease of QAF with increasing inner retinal thickness (Supplementary Table S1). Furthermore, there were significant positive correlations between QAF and the outer retina at the nasal parafovea (0.5 mm and 2.0 from foveal center) and temporal parafovea (2.5 mm from the foveal center). For data for the ETDRS grid, please see Supplementary Table S2.

Age and Outer Retinal Thickness at the Nasal Parafovea Are Predictors for QAF

Age and outer retinal thickness at the nasal parafovea (1.5 mm from foveal center) predict QAF intensity values in our cohort, $F(2, 50) = 153.4$, $P <$ 0.001. Given an intercept of 13 [QAF a.u.], each year between 5 and 18 years was attributed a QAF intensity value of 1.6 [QAF a.u.], whereas each micrometer of nasal outer retinal thickness (1.5 mm from foveal center) was attributed 0.84 [QAF a.u.]. The corrected R^2 for the overall model was 0.85, indicative of a high goodness of fit. Similar results were found using the ETDRS gird (Supplementary Table S2).

Discussion

This study reports QAF development during childhood in a large healthy Caucasian cohort. Our major findings comprise the early detection of AF at the posterior pole, an age-related increase in AF, an AF distribution at the posterior pole similar to that of adults, and correlation of AF and retinal thickness.

Earlier reports on clinical AF included QAF data from only a few healthy children.[7] Greenberg et al.[7]

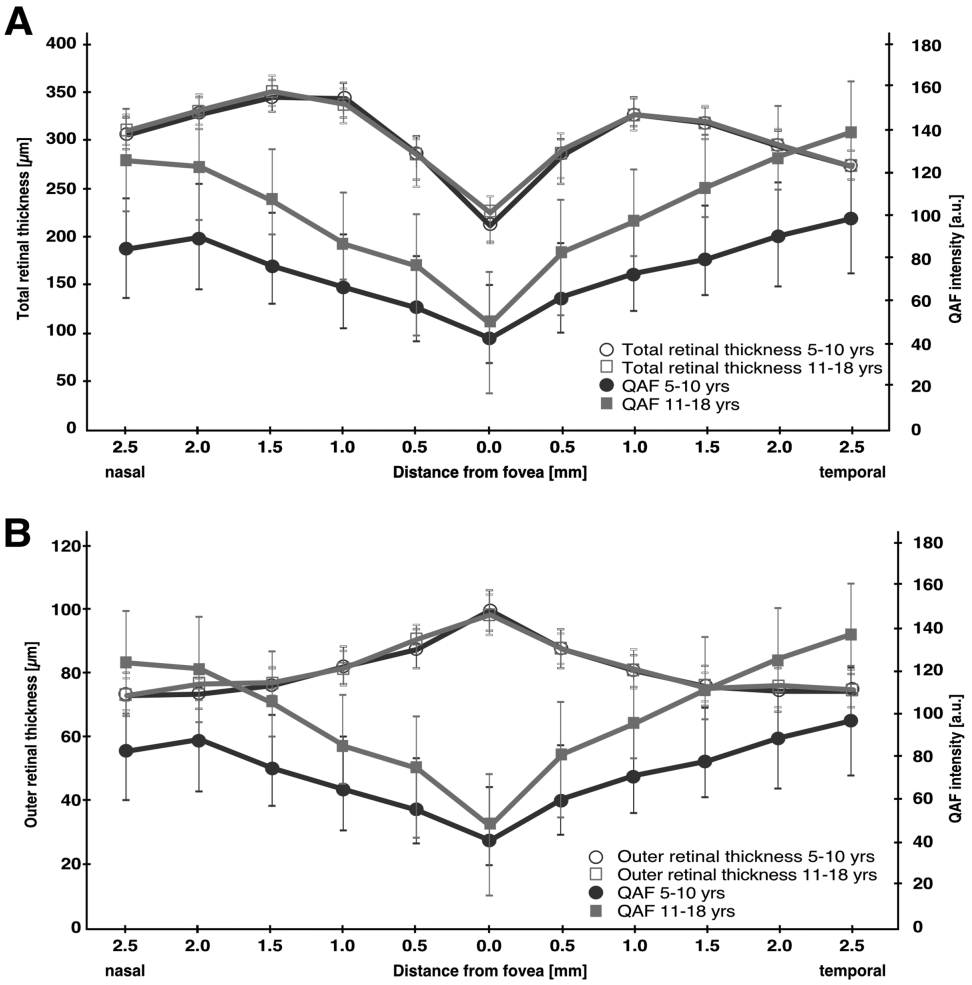

Figure 5. Correlation of retinal thickness and QAF. For both age groups, mean values with standard deviation of the corresponding QAF and retinal thickness measurements at each point of the horizontal meridian are reported. The thickness of the whole retina (between ILM and Bruch membrane) (**A**) and of the outer retinal layers (between ELM and Bruch membrane) (**B**) did not change with age. QAF values of the older children are higher compared to the younger ones. In both age groups, QAF values increased with growing distance to the fovea.

examined around 10 Caucasians, 18 Hispanics, and 8 African Americans in the age range of 5 to 20 years. Since gender might also impact QAF,[7] larger studies on QAF in healthy children are essential for a better understanding of AF development.

QAF, although still at an experimental stage, resolves the limitations of only qualitative evaluation of FAF images and enables quantitative measurements among participants and in follow-ups. Since its release in 2011,[6] QAF values have then been reported for normal aging[7] and in several retinal diseases.[12] However, previous studies reported only one QAF value for each individual eye (QAF8, mean of QAF values from eight segments at the parafoveal region), with a risk of missing information for pathologic lesions from areas outside the QAF8 ring. Also, there were no appropriate patterns for structural and other functional tests that fit the QAF8 ring pattern, which complicates adequate structural-functional testing.[13]

Structure-function correlations require measurements at the exact same locations. In this context, we recently discussed the need for alternative QAF analysis patterns that enable a more detailed analysis and correlation with other imaging modalities or functional tests at distinct posterior pole regions[8] or pathologies.[12] Our functional (QAF)–structural (retinal thickness in SD-OCT) correlation revealed that in our young cohort, increasing QAF is related to a thickening of the RPE, which parallels findings from other studies.[13] In addition, in our study, diminished QAF intensities was found with thickening of the inner retina.

Our data on retinal thickness along the horizontal meridian are comparable to other studies in children with Caucasian ethnicity.[14,15] While the thickness of

the *whole retina* nasal and temporal to the fovea did not change with age, the thickness at the foveola changed significantly, as shown in both other OCT studies and histologic studies in children´s retina.[14–17] The increase in thickness at the fovea can be explained by the elongation of the photoreceptor´s inner and outer segments and an increasing packing density until early adulthood.[18,19] Thus, the results presented support the findings of recent studies that the development of the fovea is not completed at the age 5 years, as previously assumed, but continues.[19] The QAF intensities were low at the fovea since blue light–absorbing macular pigment has its peak at the fovea.[20,21] Furthermore, the characteristic distribution of intracellular RPE granules in relation to the fovea with high amounts of melanosomes and melanolipofuscin granules at the fovea nicely explains the low QAF signals, although previously examined in adults only.[22]

In our study, outer retinal thickness (external limiting membrane to Bruch membrane distance) at the 11 points along the horizontal meridian did not change with age, which seems to contrast with findings from others, but might be related to methodologic differences.[13] Using the ETDRS grid, we also observed a thickening of the RPE/Bruch membrane complex, which could reflect the increasing accumulation of autofluorescent intracellular granules (lipofuscin, melanolipofuscin). At birth, RPE cells contain melanosomes only.[4] Histologic studies showed that during the next years of life, RPE cells accumulate autofluorescent material within melanolysosomes, while only few lipofuscin granules can be found within RPE cells of young children.[4,23] The small number of RPE lipofuscin granules nicely mirrors the low QAF signal in the youngest of our examined children. This phenomenon can be explained by the immature posterior pole at birth (RPE and photoreceptor system),[24] which then, with aging, increasing photoreceptor density, and visual cycle metabolism, leads to augmented lipofuscin and melanolipofuscin accumulation.[4,5] As the number of lipofuscin and melanolipofuscin granules increases, also QAF intensity increases. However, overall QAF intensity remains at low levels during the first two decades and does not increase until the end of the second/early third decade (Fig. 2C), also previously shown in histology.[4] In addition, an interesting finding is that young participants show a narrow QAF variability that seems to broaden in adults and the elderly (Fig. 2C).

The finding that thickening of the inner retina could lead to diminished QAF intensities reminds us that autofluorescence is not only related to the accumulation of autofluorescent granules within the RPE. Any changes in tissue transparency in the inner or outer retina (e.g., normal and pathologic tissue thickening or thinning,[25,26] accumulation of light-blocking pigments or material,[27,28] accumulation of hyperautofluorescent material,[11] and others) could lead to altered FAF, both increased and decreased, independent from the amount of the underlying autofluorescent RPE granules.

Standard retinae were generated for two age groups (5–10 and 11–18 years) and can be used for comparisons with retinal pathologies in age-matched cohorts,[29] modified as needed, and supplemented in future studies. The standard retinae reveal an increase of QAF intensities throughout the posterior pole. Noteworthy, in our cohort, the AF pattern at the posterior pole with the highest QAF signals at the temporal/temporal-superior region is identical to the pattern observed in adults.[6,8] As for adults, the reason for this increased AF signal remains speculative.

Gender-related differences in QAF with higher values in females were previously reported in a group with multiple ethnicities.[7] In our Caucasian children cohort, these gender differences were not or not yet observable. However, we were able to detect differences in retinal thickness, with boys having significantly thicker retinae compared to girls, partly in line with results from other studies in children.[14–16] In adults, these gender differences seem to be even more obvious for the whole retina.[30,31]

Limitations of our study include the cross-sectional character and the examination of each participant at one time point only, which does not allow any statements on the development of QAF in an individual. Also, the changing of axial length in the growing eye in children could affect QAF measurements.[6] Future studies following up these children could address these issues. A relatively high number of children (24%) had to be excluded due to lack of cooperation and subsequent poor QAF image quality, an issue that might be related to the young age of our participants or our strict rules for grading image quality. However, even 5-years-olds have perfectly cooperated during image acquisition. Variability in our study cohort was comparable (around 10%) to the QAF measurements in healthy adults,[7,8] which also underlines that QAF can perfectly be used for fundus imaging in children. Although interesting, it is still unclear how QAF develops in the first years of life (i.e., from birth to age 5 years). Strengths of our study include the development and use of instruments for precise structure–function correlation at exactly the same locations, a pioneer in QAF interpretation.

In conclusion, we present QAF of the largest cohort of Caucasian children so far. QAF is measurable early in life and increases with aging. The QAF distribution across the posterior pole is similar to adults,

with highest QAF intensities at the superior-temporal parafovea. While overall retinal thickness did not differ between the two age groups, a thickening of the RPE was observable, which might relate to the increasing accumulation of autofluorescent RPE granules. Future studies with the same participants can report QAF development of individual participants.

Acknowledgments

Supported by National Institutes of Health/National Eye Institute 1R01EY027948 (TA); Heidelberg Engineering provided the modified hardware for QAF imaging and technical support. The funding organizations had no role in the design and conduct of the study.

Disclosure: **C. Pröbster,** None; **I.-S. Tarau,** Novartis (R); **A. Berlin,** None; **N. Kleefeldt,** None; **J. Hillenkamp,** None; **M.M. Nentwich,** None; **K.R. Sloan,** MacRegen (I); **T. Ach,** Novarits (F, R), Roche (C), MacRegen (I)

References

1. von Ruckmann A, Fitzke FW, Bird AC. Distribution of fundus autofluorescence with a scanning laser ophthalmoscope. *Br J Ophthalmol.* 1995;79(5):407–412.
2. Delori FC, Dorey CK, Staurenghi G, Arend O, Goger DG, Weiter JJ. In vivo fluorescence of the ocular fundus exhibits retinal pigment epithelium lipofuscin characteristics. *Invest Ophthalmol Vis Sci.* 1995;36(3):718–729.
3. Sparrow JR, Yoon KD, Wu Y, Yamamoto K. Interpretations of fundus autofluorescence from studies of the bisretinoids of the retina. *Invest Ophthalmol Vis Sci.* 2010;51(9):4351–4357.
4. Feeney-Burns L, Hilderbrand ES, Eldridge S. Aging human RPE: morphometric analysis of macular, equatorial, and peripheral cells. *Invest Ophthalmol Vis Sci.* 1984;25(2):195–200.
5. Ach T, Huisingh C, McGwin G, Jr, et al. Quantitative autofluorescence and cell density maps of the human retinal pigment epithelium. *Invest Ophthalmol Vis Sci.* 2014;55(8):4832–4841.
6. Delori F, Greenberg JP, Woods RL, et al. Quantitative measurements of autofluorescence with the scanning laser ophthalmoscope. *Invest Ophthalmol Vis Sci.* 2011;52(13):9379–9390.
7. Greenberg JP, Duncker T, Woods RL, Smith RT, Sparrow JR, Delori FC. Quantitative fundus autofluorescence in healthy eyes. *Invest Ophthalmol Vis Sci.* 2013;54(8):5684–5693.
8. Kleefeldt N, Bermond K, Tarau IS, et al. Quantitative fundus autofluorescence: advanced analysis tools. *Transl Vis Sci Technol.* 2020;9(8):2.
9. Burke TR, Duncker T, Woods RL, et al. Quantitative fundus autofluorescence in recessive Stargardt disease. *Invest Ophthalmol Vis Sci.* 2014;55(5):2841–2852.
10. Gliem M, Müller PL, Finger RP, McGuinness MB, Holz FG, Charbel Issa P. Quantitative fundus autofluorescence in early and intermediate age-related macular degeneration. *JAMA Ophthalmol.* 2016;134(7):817–824.
11. Duncker T, Greenberg JP, Ramachandran R, et al. Quantitative fundus autofluorescence and optical coherence tomography in best vitelliform macular dystrophy. *Invest Ophthalmol Vis Sci.* 2014;55(3):1471–1482.
12. Reichel C, Berlin A, Radun V, et al. Quantitative fundus autofluorescence in systemic chloroquine/hydroxychloroquine therapy. *Transl Vis Sci Technol.* 2020;9(9):42.
13. Cozzi M, Viola F, Belotti M, et al. The in vivo correlation between retinal pigment epithelium thickness and quantitative fundus autofluorescence in a Caucasian population [published online August 5, 2020]. *Ophthalmol Retina.*
14. Turk A, Ceylan OM, Arici C, et al. Evaluation of the nerve fiber layer and macula in the eyes of healthy children using spectral-domain optical coherence tomography. *Am J Ophthalmol.* 2012;153(3):552–559.e551.
15. Yanni SE, Wang J, Cheng CS, et al. Normative reference ranges for the retinal nerve fiber layer, macula, and retinal layer thicknesses in children. *Am J Ophthalmol.* 2013;155(2):354–360.e351.
16. Eriksson U, Holmström G, Alm A, Larsson E. A population-based study of macular thickness in full-term children assessed with Stratus OCT: normative data and repeatability. *Acta Ophthalmol.* 2009;87(7):741–745.
17. Lee H, Purohit R, Patel A, et al. In vivo foveal development using optical coherence tomography. *Invest Ophthalmol Vis Sci.* 2015;56(8):4537–4545.
18. Hendrickson AE, Yuodelis C. The morphological development of the human fovea. *Ophthalmology.* 1984;91(6):603–612.
19. Hendrickson A, Possin D, Vajzovic L, Toth CA. Histologic development of the human fovea

from midgestation to maturity. *Am J Ophthalmol.* 2012;154(5):767–778.e762.
20. Snodderly DM, Brown PK, Delori FC, Auran JD. The macular pigment, I: absorbance spectra, localization, and discrimination from other yellow pigments in primate retinas. *Invest Ophthalmol Vis Sci.* 1984;25(6):660–673.
21. Bone RA, Landrum JT, Fernandez L, Tarsis SL. Analysis of the macular pigment by HPLC: retinal distribution and age study. *Invest Ophthalmol Vis Sci.* 1988;29(6):843–849.
22. Bermond K, Wobbe C, Tarau IS, et al. Autofluorescent granules of the human retinal pigment epithelium: phenotypes, intracellular distribution, and age-related topography. *Invest Ophthalmol Vis Sci.* 2020;61(5):35.
23. Feeney L. Lipofuscin and melanin of human retinal pigment epithelium: fluorescence, enzyme cytochemical, and ultrastructural studies. *Invest Ophthalmol Vis Sci.* 1978;17(7):583–600.
24. Hendrickson A. A morphological comparison of foveal development in man and monkey. *Eye.* 1992;6(2):136–144.
25. von Ruckmann A, Fitzke FW, Bird AC. In vivo fundus autofluorescence in macular dystrophies. *Arch Ophthalmol.* 1997;115(5):609–615.
26. Bertolotto M, Borgia L, Iester M. Hyperautofluorescence in outer retinal layers thinning. *Biomed Res Int.* 2014;2014:741538.
27. Rothenbuehler SP, Wolf-Schnurrbusch UE, Wolf S. Macular pigment density at the site of altered fundus autofluorescence. *Graefes Arch Clin Exp Ophthalmol.* 2011;249(4):499–504.
28. Lee CS, Lee AY, Forooghian F, Bergstrom CS, Yan J, Yeh S. Fundus autofluorescence features in the inflammatory maculopathies. *Clin Ophthalmol.* 2014;8:2001–2012.
29. Lorenz B, Wabbels B, Wegscheider E, Hamel CP, Drexler W, Preising MN. Lack of fundus autofluorescence to 488 nanometers from childhood on in patients with early-onset severe retinal dystrophy associated with mutations in RPE65. *Ophthalmology.* 2004;111(8):1585–1594.
30. Kashani AH, Zimmer-Galler IE, Shah SM, et al. Retinal thickness analysis by race, gender, and age using Stratus OCT. *Am J Ophthalmol.* 2010;149(3):496–502.e491.
31. Wong A, Chan C, Hui S. Relationship of gender, body mass index, and axial length with central retinal thickness using optical coherence tomography. *Eye.* 2005;19(3):292–297.